THE SZEWALSKI INSTITUTE OF FLUID-FLOW MACHINERY
POLISH ACADEMY OF SCIENCES

TRANSACTIONS OF THE INSTITUTE OF FLUID-FLOW MACHINERY

115

GDAŃSK 2004

TRANSACTIONS OF THE INSTITUTE OF FLUID-FLOW MACHINERY
Appears since 1960

Aims and Scope

Transactions of the Institute of Fluid-Flow Machinery have primarily been established to publish papers from four disciplines represented at the Institute of Fluid-Flow Machinery of Polish Academy of Sciences, such as:

- Liquid flows in hydraulic machinery including exploitation problems,
- Gas and liquid flows with heat transport, particularly two-phase flows,
- Various aspects of development of plasma and laser engineering,
- Solid mechanics, machine mechanics including exploitation problems.

The periodical, where originally were published papers describing the research conducted at the Institute, has now appeared to be the place for publication of works by authors both from Poland and abroad. A traditional scope of topics has been preserved.

Only original and written in English works are published, which represent both theoretical and applied sciences. All papers are reviewed by two independent referees.

EDITORIAL AND PUBLISHING OFFICE

IFFM Publishers (Wydawnictwo IMP), Institute of Fluid Flow Machinery, Fiszera 14, 80-952 Gdańsk, Poland, Tel.: +48(58)3411271 ext. 141, Fax: +48(58)3416144, E-mail: esli@imp.gda.pl http://www.imp.gda.pl/

Terms of subscription

Subscription order and payment should be directly sent to the Publishing Office

Warunki prenumeraty w Polsce

Wydawnictwo ukazuje się przeciętnie dwa lub trzy razy w roku. Cena numeru wynosi 20,- zł + 5,- zł koszty wysyłki. Zamówienia z określeniem okresu prenumeraty, nazwiskiem i adresem odbiorcy należy kierować bezpośrednio do Wydawcy (Wydawnictwo IMP, Instytut Maszyn Przepływowych PAN, ul. Gen. Fiszera 14, 80-952 Gdańsk). Osiągalne są również wydania poprzednie. Prenumerata jest również realizowana przez jednostki kolportażowe RUCH S.A. właściwe dla miejsca zamieszkania lub siedziby prenumeratora. W takim przypadku dostawa następuje w uzgodniony sposób.

ISSN 0079-3205

TRANSACTIONS OF THE INSTITUTE OF FLUID-FLOW MACHINERY

No. 115, 2004, 69-81

JAROSŁAW W. FRĄCZAK*and EUSTACHY S. BURKA

Simulation of incompressible flow past a bluff cylinder by means of a discrete vortex method

The Szewalski Institute of the Fluid Flow Machinery of the Polish Academy of Sciences, 80-952 Gdańsk, ul J. Fiszera14, PO Box 621, Poland

Abstract

A two-dimensional viscous, incompressible, unsteady flow past a bluff cylinder with sharp edges is simulated using a purely deterministic Lagrangian model incorporating viscous effects (diffusion and no-slip boundary condition). The method applied is based on a combination of the discrete vortex and the panel method. The viscous diffusion effect is simulated by means of the diffusion velocity method. The evolution of vortical flow past a square cylinder after its impulsive start and motion with constant velocity in resting liquid is simulated for moderate Reynolds numbers and several different angles of incidence.

Keywords: Unsteady viscous flow; Numerical simulation; Discrete vortex method

Nomenclature

b	–	half length of the cylinder side
f_s	–	shape function
t	–	time
s	–	distance along a boundary
u_s	–	tangential velocity
k, n	–	unit vectors
u	–	velocity vector
x	–	position vector
D	–	fluid flow region
F	–	smoothing function
N	–	number of discrete vortices
M	–	number of control points
Re	–	Reynolds number

*Corresponding author. E-mail address: jfrk@imp.gda.pl

$\boldsymbol{R}^2$ – two-dimensional Euclidean space
Δt – time step
Δs – length of a segment
α – angle of incidence
∂D – boundary of flow region
ε – distance from the wall
γ – strength of vortex sheet
λ – strength of a vortex, circulation
ν – kinematic viscosity
σ – smoothing parameter
ω – vorticity
Γ – strength of a vortex, circulation
∇ – gradient operator

1 Introduction

A bluff body is featured by a non-streamlined geometry, responsible for flow unsteadiness involving massive boundary layer separations and a wake of substantial cross-section. This paper presents a numerical model based on a discrete vortex approach which has been used to simulate a two-dimensional, viscous, incompressible time-dependent flow past a bluff, sharp edged body, such as a rectangular cylinder. Despite simple geometrical conditions, determination of the flow past such a body is a complex task, dealt with in numerous experimental and numerical studies. The model applied in this paper refers to those described among others in [1-5]. The approach adopted combines the discrete vortex method with the panel (boundary element) and the diffusion velocity methods. It provides a grid-free approach to model vortical viscous flows past solid bodies. The paper presents a brief overview of the modelling technique fundamentals and some initial results on the flow past a square cylinder impulsively started from the standstill to a uniform motion. The flow is studied in a frame of reference fixed to the cylinder.

1.1 Basic vorticity formulations

The motion of an incompressible fluid in a two-dimensional domain $D \subset \boldsymbol{R}^2$, internally bounded by ∂D (∂D corresponds to the solid body surface), is defined in terms of vorticity by the equation of vorticity transport and the condition that the velocity field is divergence-free:

$$\frac{\partial \omega}{\partial t} + (\boldsymbol{u} \cdot \nabla)\omega = \frac{1}{\mathrm{Re}} \nabla^2 \omega, \tag{1}$$

$$\nabla \cdot \boldsymbol{u} = 0, \tag{2}$$

where $\boldsymbol{u} = \boldsymbol{u}(\boldsymbol{x}, t)$ is the fluid velocity, $\boldsymbol{x} \in \boldsymbol{R}^2$ is the position vector, $t > 0$ is time and Re is the Reynolds number. The vorticity $\omega = \omega(\boldsymbol{x}, t)$ of the flow field is defined by the equation:

$$\omega \boldsymbol{k} = \nabla \times \boldsymbol{u}, \tag{3}$$

where $\boldsymbol{k}$ is a unit vector normal to the flow field plane. The flow field satisfies the following boundary conditions

$$\boldsymbol{u} = 0 \text{ at } \partial D; \qquad \boldsymbol{u}(\boldsymbol{x}, t) \to \boldsymbol{u}_\infty \text{ as } |x| \to \infty \tag{4}$$

and the initial condition

$$\boldsymbol{u}(\boldsymbol{x}, 0) \text{ given for } \boldsymbol{x} \in D. \tag{5}$$

Kinematic relationship between the velocity and vorticity fields is defined by the generalized Biot-Savart law [6,7] applied to the flow area bounded by ∂D

$$\boldsymbol{u}(\boldsymbol{x}) = \frac{1}{2\pi} \int_D \frac{\omega(\boldsymbol{x}')\boldsymbol{k} \times (\boldsymbol{x} - \boldsymbol{x}')}{|\boldsymbol{x} - \boldsymbol{x}'|^2} d\boldsymbol{x}' - \frac{1}{2\pi} \oint_{\partial D} \frac{(\boldsymbol{n} \times \boldsymbol{u}_0) \times (\boldsymbol{x} - \boldsymbol{x}'(s))}{|\boldsymbol{x} - \boldsymbol{x}'(s)|^2} ds + \boldsymbol{u}_\infty, \tag{6}$$

where $\boldsymbol{n}$ is the outward unit vector normal to the ∂D boundary, $\boldsymbol{u}_0$ is velocity at the boundary, $\boldsymbol{u}_\infty$ denotes velocity of the uniform free stream at infinity, s is the distance measured along the boundary and $\boldsymbol{x}'(s)$ is the positioning vector of the relevant point at the boundary. The boundary integral accounts for the vorticity distribution on the ∂D boundary. The contribution from source distribution on the boundary is omitted here. For given vorticity distributions in the flow field, the specific strength of the vortex sheet on the boundary is obtained from Eq. (6) applied to points $\boldsymbol{x}(s)$ located on the boundary [8]. This leads to the Fredholm type integral equation:

$$\oint_{\partial D} \frac{\gamma(s')\boldsymbol{k} \times (\boldsymbol{x}(s) - \boldsymbol{x}(s'))}{|\boldsymbol{x}(s) - \boldsymbol{x}(s')|^2} ds' = \boldsymbol{U}(\boldsymbol{x}(s)) + 2\pi(\boldsymbol{u}(\boldsymbol{x}(s)) - \boldsymbol{u}_\infty), \tag{7}$$

where γ is the vortex sheet strength. The $\boldsymbol{U}(x(s))$ vector represents velocity induced by the vorticity in the fluid and $\boldsymbol{u}(\boldsymbol{x}(s))$ is defined by the velocity boundary values. The uniqueness of Eq. (7) solution requires fulfilment of the principle of total vorticity conservation in both the fluid and solid domains:

$$\frac{d}{dt} \int_{D \cup \partial D} \omega(\boldsymbol{x}) d\boldsymbol{x} = 0 \tag{8}$$

which implies that the circulation around a contour far from the body remains constant (Kelvin circulation theorem). Consequently, if total vorticity is initially zero, it remains zero also later on.

Let the half-length of the square cylinder cross-section side, b, and the value of upstream uniform flow velocity, u_∞, represent the reference length and flow velocity, respectively. All quantities were non-dimensionalised as follows: $\boldsymbol{x}' = \boldsymbol{x}/b$, $t' = tu_\infty/b$, $\boldsymbol{u}' = \boldsymbol{u}/u_\infty$, $\Gamma' = \Gamma/u_\infty b$, $\gamma' = \gamma/u_\infty$, $\omega' = \omega b/u_\infty$, $\mathrm{Re} = bu_\infty/\nu$. For the sake of simplicity, the superscript primes are dropped from the dimensionless quantities in the considerations.

2 Discrete vortex method

The vortex methods are derived and analyzed in many references [7,9-12], so only a brief description of the method is provided herein.

It follows from Eq. (1) that in an inviscid case ($\mathrm{Re} = \infty$) the vorticity associated with fluid elements remains constant along their trajectories. The essence of the vortex method is to discretise the vorticity field by means of the equation:

$$\omega(\boldsymbol{x}, t) = \sum_{i=1}^{N} \Gamma_i f_\sigma(\boldsymbol{x} - \boldsymbol{x}_i(t)) \tag{9}$$

such that

$$\sum_{i=1}^{N} \Gamma_i = \int_D \omega(\boldsymbol{x}) d\boldsymbol{x}, \tag{10}$$

where Γ_i is the strength (circulation) of the $i-$th discrete vortex located at point $\boldsymbol{x}_i = \boldsymbol{x}_i(t)$ at time t, N is number of vortices and f_σ is the shape function approximating the Dirac δ – function. The shape function, usually radially symmetric, represents vorticity distribution due to a discrete vortex and is selected so that

$$f_\sigma(\boldsymbol{x}) = \frac{1}{\sigma^2} f\left(\frac{|\boldsymbol{x}|}{\sigma}\right), \tag{11}$$

with a 2D normalization

$$\int_{R^2} f(\boldsymbol{x}) d\boldsymbol{x} = 1, \tag{12}$$

where σ is a smoothing parameter.

To satisfy the vorticity convection equation, the velocity of each vortex must be given by the value of the velocity field at its actual location. The trajectories of discrete vortices are approximated by a solution of the following Cauchy problem

$$\frac{d\Gamma_i}{dt} = 0, \tag{13}$$

$$\frac{d\boldsymbol{x}_i}{dt} = \boldsymbol{u}(\boldsymbol{x}_i, t), \quad \boldsymbol{x}_i(t_0) = \boldsymbol{x}_{i0}, \tag{14}$$

with $i = 1, .., N$. The velocity induced at $\boldsymbol{x}_i(t)$, by system of discrete vortices is defined as:

$$\boldsymbol{u}(\boldsymbol{x}_i, t) = -\frac{1}{2\pi} \sum_{j=1}^{N} \Gamma_j \frac{(\boldsymbol{x}_i - \boldsymbol{x}_j) \times \boldsymbol{k}}{|\boldsymbol{x}_i - \boldsymbol{x}_j|^2} F\left(\frac{|\boldsymbol{x}_i - \boldsymbol{x}_j|}{\sigma}\right), \tag{15}$$

with

$$F(\zeta) = 2\pi \int_0^{\zeta} f_\sigma(s) s ds, \quad \zeta = \frac{r}{\sigma}, \tag{16}$$

where $r = |\boldsymbol{x} - \boldsymbol{x}_j|$. In the case of the shape function of Gaussian type [9], which is used here, the smoothing function for the Biot-Savart integral is

$$F(\zeta) = 1 - e^{-\frac{\zeta^2}{\sigma^2}}. \tag{17}$$

In this study, the above system of ordinary differential equations is solved numerically using the Euler time integration scheme of the first order:

$$\boldsymbol{x}_i^{k+1} = \boldsymbol{x}_i^k + \boldsymbol{u}(\boldsymbol{x}_i^k)\Delta t + O(\Delta t^2), \tag{18}$$

where Δt is the time step, k denotes the k^{th} time step, $t_k = k\Delta t$, and $\boldsymbol{x}_i^k = \boldsymbol{x}_i(t_k)$ is the position of the i^{th} discrete vortex at the k^{th} time step.

3 Diffusion velocity method

The purely Lagrangian diffusion velocity method is based on application of Fick's law to the vorticity flux [13]. After some transformations Eq. (1) takes the following form:

$$\frac{\partial \omega}{\partial t} + \nabla \cdot (\omega \boldsymbol{u}_c - \omega \frac{1}{\mathrm{Re}\,\omega} \nabla \omega) = 0, \tag{19}$$

where $\boldsymbol{u}_c$ denotes the convection velocity. Considering

$$\boldsymbol{u}_d = -\frac{1}{\mathrm{Re}\,\omega} \nabla \omega, \tag{20}$$

as the diffusion velocity, Eq. (19) can be rewritten as

$$\frac{\partial \omega}{\partial t} + \nabla \cdot [\omega(\boldsymbol{u}_c + \boldsymbol{u}_d)] = 0. \tag{21}$$

Hence, the effect of viscosity is taken into account by adding the diffusion velocity to the convection velocity of each vortex and the right hand side of the ordinary

differential equations of discrete vortex motion is complemented by the term representing diffusion velocity

$$\frac{d\boldsymbol{x}_i}{dt} = \boldsymbol{u}_c(\boldsymbol{x}_i, t) + \boldsymbol{u}_d(\boldsymbol{x}_i, t), \quad \boldsymbol{x}_i(t_0) = \boldsymbol{x}_{i0}. \tag{22}$$

According to the discrete vortex approach, the diffusion velocities, as well as vorticity distribution, are expressed by a sum of contributions of all the vortices

$$\boldsymbol{u}_d(\boldsymbol{x}_i, t) = \frac{2}{\pi\sigma^4 \mathrm{Re}\ \omega_i} \sum_{j=1}^{N} \Gamma_j (\boldsymbol{x}_i - \boldsymbol{x}_j) \exp\left(-\frac{|\boldsymbol{x}_i - \boldsymbol{x}_j|^2}{\sigma^2}\right). \tag{23}$$

where

$$\omega_i = \frac{1}{\pi\sigma^2} \sum_{j=1}^{N} \Gamma_j \exp\left(-\frac{|\boldsymbol{x}_i - \boldsymbol{x}_j|^2}{\sigma^2}\right). \tag{24}$$

4 Boundary conditions

Due to the inviscid impermeability and the viscous no-slip conditions the flow velocity vanishes at the solid boundary. While the impermeability condition can be satisfied approximately by potential flow cancelling the normal velocity component at the boundary within the panel method [14,15], the no-slip condition is satisfied by generating new vorticity on the surface of the body and introducing it into the flow field in order to simulate the physical process of vorticity creation in the real flow [16,17].

4.1 Normal boundary condition

In order to obtain the vortex distribution at the ∂D boundary, the contour of the body is divided into M short straight-line segments or panels and some distribution of vortex singularities is assumed at each panel. The impermeability boundary condition applied at control points, placed at mid-points of the segments, and the Kelvin theorem, Eq. (8), constitutes a system of linear algebraic equations with unknown values of vortex strength γ_j

$$\sum_{j=1}^{M} a_{ij}\gamma_j = b_i, \quad i = 1, ..., M+1. \tag{25}$$

The a_{ij} coefficients are elements of the transfer matrix representing normal velocity component at the i-th panel induced by the j-th panel vorticity. The components b_i of the rhs vector are the normal velocities at the i-th panel control

point induced by free vortices in the flow area and by the uniform stream. For the purpose of this study, the $\gamma(s)$ distribution at the boundary is approximated by the resultant singularity vortices of strength λ_i placed at panel junction points. The last equation in the system of linear equations (25), represents the total vorticity in the flow system and can be reduced to the form:

$$\sum_{i=1}^{M} \lambda_i + \sum_{i=1}^{N} \Gamma_i = 0. \tag{26}$$

The system of $M+1$ equations with M unknowns is overdetermined. The straightforward method to solve such a system is to ignore one equation, e.g. the equation describing the impermeability condition at a control point of minor significance, usually in the central part of the streamlined body rear surface.

4.2 Tangential boundary condition

To model the vorticity diffusion from the solid surface, the vortex sheet corresponding to the no-slip condition is partitioned into vortex sheet elements centred at the control points. Then the vortex sheet elements are replaced by discrete vortices, which are inserted into the flow field close to the streamlined surface. The strength of these vortex sheet elements is equal to the tangential velocity of the flow relative to the solid wall.

Assuming constant vorticity within each element, the strength of generated vortices can be considered equal to the total vorticity of the relevant vortex sheet elements

$$\Gamma_i = \gamma_i \cdot \Delta s = -u_{si} \Delta s, \quad i = 1, ..., M, \tag{27}$$

where u_{si} is tangential velocity of the flow at the i-th control point and Δs is the length of the relevant vortex sheet segment.

There is no rigorous criterion to determine the distance between the solid wall and the position where newly created vortices should be introduced into the flow field. In this study, new vortices are placed at creation points situated in front of the control points. The distance between the vortex generation points and the boundary is assumed to be equal to the smoothing parameter and slightly larger than panel length, that is $1.08\Delta s$.

5 Computational procedure

The simulation process of the vortex flow evolution in each time step consists in the following operations:

1. Determination of the vortex distribution over panels satisfying the impermeability and the circulation conservation conditions.
2. Calculation of the convection and diffusion velocities of each discrete vortex.
3. Computation of the tangential velocities at the panels and creation of new discrete vortices.
4. Introduction of a series of new discrete vortices along the contour.
5. Displacement of all discrete vortices according to the velocity distribution.

Whenever a discrete vortex already in the flow crosses the contour of the body, it is 'reflected' back into the flow field. Also for computational reasons, in calculations of the diffusing velocities, Eq. (23), discrete vortices with opposite sense of circulation were treating separately to avoid producing unreasonably large velocities, [18].

6 Results and discussion

The evolution of a vortical unsteady flow past a square cylinder moving with constant velocity in still liquid has been simulated for Reynolds numbers ($\mathrm{Re} = bu_\infty/\nu$) 10^3 and 10^4 with three different angles of attack ($b = 1$ and $u_\infty = 1$ for this study). The starting point for the evolution was the potential flow formed immediately after an impulsive start of the cylinder. The dimensionless integration time step was set at $\Delta t' = \Delta t b/u_\infty = 0.05$. The surface of rectangular cylinder was represented by $M = 128$ equal panels of length $\Delta s = 0.0625\,b$. The distance between the free vortex creation points and the body wall was $\varepsilon' = \varepsilon/b = 0.07$. The radius of smoothing parameter was $\sigma' = \sigma/b = 0.07$ (0.035 of the body size). Some initial qualitative results of simulations carried out are presented here.

The development of the wake behind a square cylinder for angle of flow incidence $\alpha = 20°$ at Reynolds number $\mathrm{Re} = 10^4$ is shown in Fig. 1. Discrete vortex distributions at dimensionless time $t = 5, 10, 15$ and 20 after an impulsive start illustrate the growth of vortex structures in the wake in the course of time. At every moment there is an intense concentration of discrete vortices in the vicinity of the body to be stated. After preliminary clustering of discrete vortices, a large vortex structure develops. At the beginning, the starting vortex is created close to the rear side. Afterwards, alternate large scale vortex formations occur. In Fig. 2, a similar sequence of wake development is shown for the same time points and inflow stream direction, but with a smaller Reynolds number, $\mathrm{Re} = 10^3$. Although flow detachment takes place at the same fixed points as in the case of $\mathrm{Re} = 10^4$, which is usual for flow past sharp edged obstacles, the comparison of

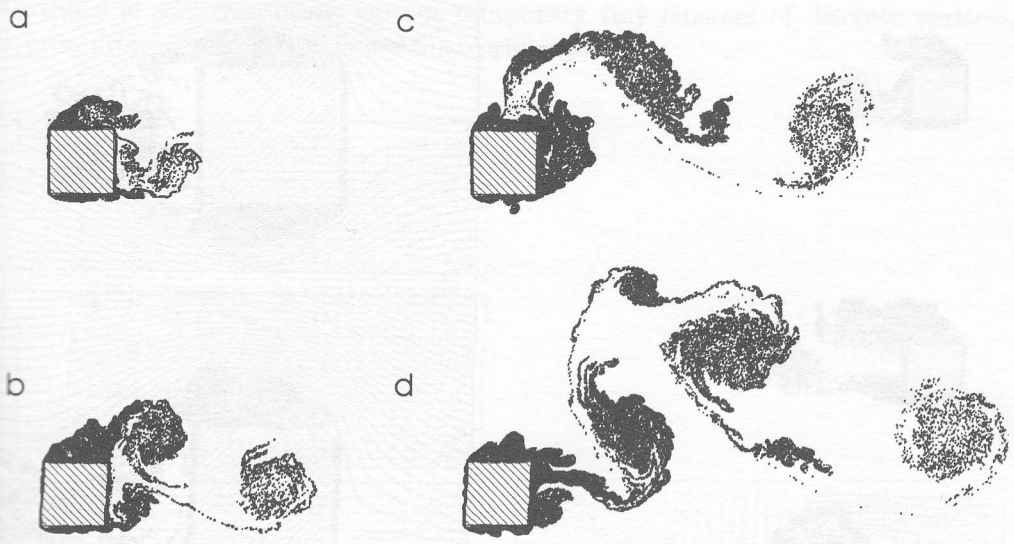

Figure 1. *Development of the vortical wake behind a square cylinder after an impulsive start* from rest at dimensionless time t: a. 5, b. 10, c. 15 and d. 20, for angle of flow incidence $\alpha = 20^\circ$ and $\mathrm{Re} = 10^4$.

Figs. 1 and 2 shows, there is a slight difference in the structure of separation regions and large scale vortices. The effect of Reynolds number on the flow pattern is revealed here in form of discrete vortices distribution. The clusters of vortices are more widely spread at lower Reynolds numbers. The details of flow pattern at initial stage of its development for three different angles of flow incidence, $\alpha = 0^\circ$, 10° and 20°, at Reynolds number $\mathrm{Re} = 10^4$ are compared in Fig. 3. By comparing vortex distributions and instantaneous streamlines at dimensionless time $t = 5$ one can see the essential difference in the early stage of wake evolution between the case of zero angle of flow incidence and the other configurations.

In the case of zero angle of incidence, a symmetrical detachment takes place at the front edges and two vortex separation regions develop along cylinder sides. The discrete vortices progressively concentrate behind body forming pairs of clusters, which grow up downstream of the obstacle while remaining symmetrical in respect to the wake axis. This initial formation of two symmetric vortices behind the cylinder is evident from the velocity vector fields plotted in Fig. 4. In contrary to the above, at larger angles of incidence the flow pattern shows full asymmetry and only one large scale vortex is formed behind the cylinder. For-

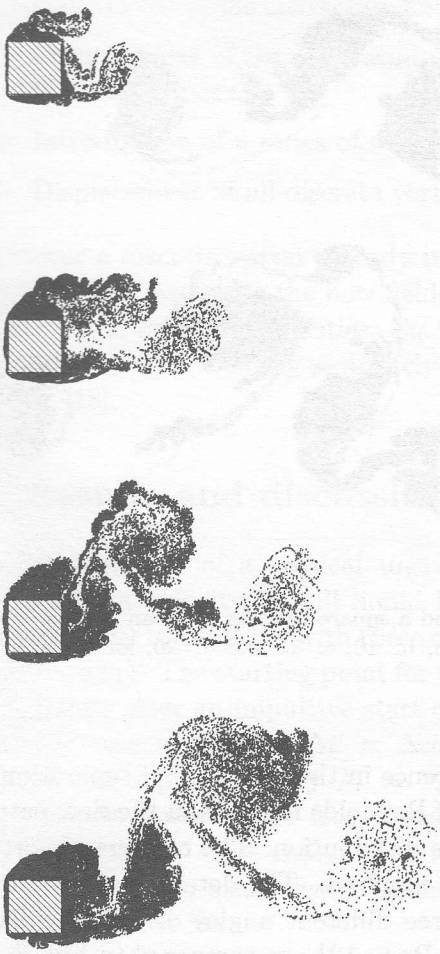

Figure 2. Development of the vortical wake behind a square cylinder after an impulsive start from rest at dimensionless time $t = 5$, 10, 15 and 20, for angle of flow incidence $\alpha = 20°$ and $\mathrm{Re} = 10^3$.

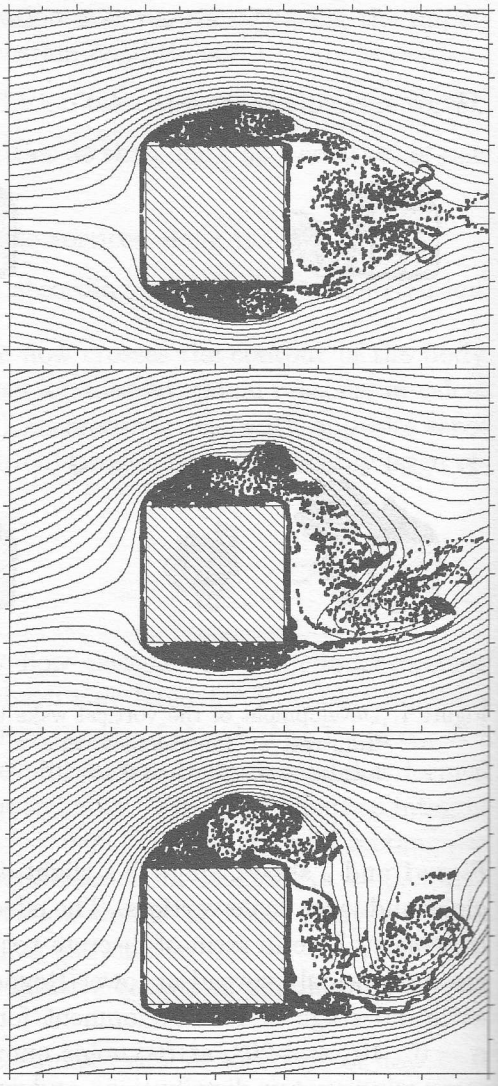

Figure 3. Flow patterns (discrete vortex distributions and instantaneous streamlines) around a square cylinder at time $t = 5$ with $\mathrm{Re} = 10^4$ for angles of flow incidence $\alpha = 0°$, 10° and 20°.

mation and development of such a vortex is shown also in the velocity plot in Fig. 4. The shear flow behind the front bottom edge reattaches to the side face of the cylinder and finally separates from the rear edge. Discrete vortices, which

approximate this shear layer just downstream the edge, continue their motion in direction tangential to the side face. Moreover, at separation regions near to the side and rear faces, various temporary tiny clusters of discrete vortices, representing recirculating flow zones, originate.

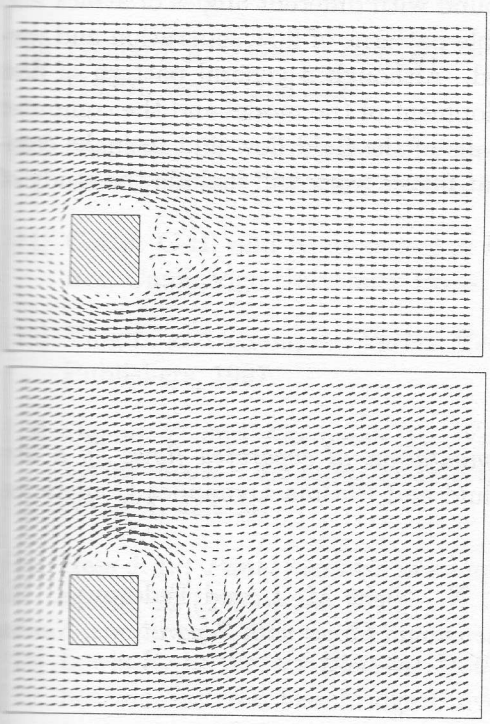

Figure 4. Velocity vectors of the flow around a square cylinder after an impulsive start from rest at time $t = 5$ with $\mathrm{Re} = 10^4$ for angles of flow incidence $\alpha = 0°$ and $20°$.

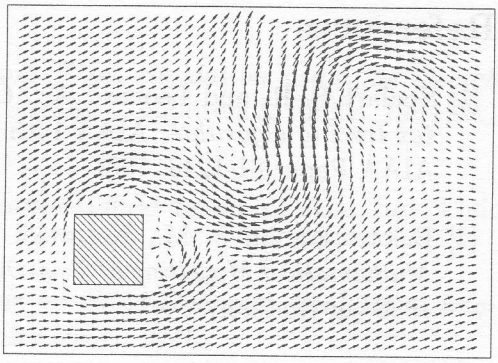

Figure 5. Velocity vectors of the flow around a square cylinder after an impulsive start from rest at time $t = 20$ with $\mathrm{Re} = 10^4$ for angle of flow incidence $\alpha = 20°$.

The vector velocity field formed at dimensionless time $t = 20$ in case of the incidence angle $\alpha = 20°$ is shown in Fig. 5. This velocity field corresponds to the discrete vortex distribution shown at the bottom of Fig. 1. It is characterized by asymmetrical flow separations from the edges of the cylinder and by flow velocity almost tangential to the bottom face. As was the case in Fig. 4, intense recirculation regions in the wake are clearly visible. Single recirculation zone, behind the body, leading to formation of a large scale eddy in the nearby wake and the previously formed vortices with staggered pattern downstream in the wake are also easily distinguishable.

7 Summary

A numerical model, based on a combination of the vortex method, diffusion velocity and panel methods, has been applied to simulate a two-dimensional unsteady, incompressible, viscous separated flow past a bluff body. Calculation was carried out for a square cylinder flown around with different angles of attack and at moderate Reynolds numbers. Reasonable patterns of flow separation and vortical wake development have been derived. Although a general pattern of flow evolution is well reproduced, further development of the model and the computer code are necessary to better simulate details of the fluid flow and to make computations more efficient. It is assumed that future work will include the study of more elongated rectangular cylinders.

Received 5 November 2003

References

[1] Spalart P. R. and Leonard A.: *Computation of separated flows by a vortex tracing algorithm*, AIAA 14th Fluid and Plasma Dynamics Conference, AIAA Paper 81-1246, 1981.

[2] Belotserkovskii S. M., Kotovskii V. N., Nisht M. I. and Fedorov R. M.: *Mathematical Modelling of Two-Dimensional Flows with Separations*, Nauka, 1988 (in Russian).

[3] Inamuro T., Adachi T. and Sakata H.: *A numerical analysis of unsteady separated flow by vortex shedding model*, Bull. JSME, 26 (1983), No. 222, 2106-2112.

[4] Sarpkaya T. and Ihring C. J.:*Impulsively started flow about rectangular prisms: experiments and discrete vortex analysis*, ASME J. Fluids Eng., 108 (1986), No. 1, 47-54.

[5] Otsuka M., Kida T., Wada M. and Kurata M.: *Two-dimensional transient flows around a rectangular cylinder by a vortex method*, Selected Papers 1st Int. Conf. on Vortex Methods, eds. Kamemoto, K., and Tsutahara, M., World Sci. Publ. Co. Pte. Ltd, 2000, 50-56.

[6] Wu J. C. and Thompson J. F.: *Numerical solution of time-dependent incompressible Navier-Stokes equations using an integro-differential formulation*, Computers & Fluids, 1 (1973), No. 2, 197-215.

[7] Kamemoto K.: *On attractive features of the vortex methods*, Computational Fluid Dynamics Review 1995, ed. M. Hafez and K. Oshima, John Wiley & Sons, 1995, 334-353.

[8] Wu J. C. and Gulcat U.: *Separate treatment of attached and detached flow regions in general viscous flows*, AIAA J., 19 (1981), No. 1, 20-27.

[9] Leonard A.: *Vortex methods for flow simulation*, J. Comput. Physics, 37 (1980), No. 3, 289-335.

[10] Sarpkaya T.: *Computational methods with vortices – the 1988 Freeman scholar lecture*, ASME J. Fluids Eng., 111 (1989), No. 1, 5-52.

[11] Cottet G-H. and Koumoutsakos P. D.: *Vortex Methods: Theory and Practice*, Cambridge University Press, 2000.

[12] Ying L. and Zhang P.: *Vortex Methods*, Science Press and Kluwer Academic Publishers, 1997.

[13] Ogami Y. and Akamatsu T.: *Viscous fFlow simulation using the discrete vortex model – the diffusion velocity method*, Computers & Fluids, 19 (1991), No. 3/4, 433-441.

[14] Hess J. L.: *Panel methods in computational fluid dynamics*, Ann. Rev. Fluid Mech., 22 (1990), 255-274.

[15] Lewis R. I.: *Vortex Element Methods for Fluid Dynamic Analysis of Engineering Systems*, Cambridge University Press, 1991.

[16] Chorin A. J.: *Numerical study of slightly viscous flow*, J. Fluid Mech., 57 (1973), Part 4, 785-796.

[17] Lewis R. I.: *Surface vorticity modelling of separated flows from two-dimensional bluff bodies of arbitrary shape*, J. Mech. Eng. Sci., 23 (1981), No. 1, 1-12.

[18] Ogami Y.: *Vortex method for heat-vortex interaction and fast summation technique*, Selected Papers 1st Int. Conf. on Vortex Methods, eds. Kamemoto, K., and Tsutahara, M., World Sci. Publ. Co. Pte. Ltd, 2000, 145-152.